Diffusion in CaCO3 Calcite Investigated by Atomic-Scale Simulations

Rémy Besson, David Tingaud, Loïc Favergeon

Diffusion in $CaCO_3$ Calcite Investigated by Atomic-Scale Simulations

Rémy Besson,* ,† David Tingaud,‡ and Loïc Favergeon §

† Groupe de Métallurgie Physique et Génie des Matériaux, Unité Matériaux et Transformations, CNRS UMR 8207, Université de Lille, F-59655 Villeneuve d ' Ascq, France

‡ Laboratoire des Sciences des Procédés et des Matériaux, CNRS UPR 3407, Institut Galilée, Université Paris XIII, 99 Avenue Jean-Baptiste Clément, F-93430 Villetaneuse, France

§ Mines Saint-Etienne, Université de Lyon, CNRS, UMR 5307, LGF, centre SPIN, F-42023 Saint-Etienne, France

ABSTRACT: In the context of CO_2 storage, we used ab initio-based atomic-scale modelings and simulations to study oxygen and carbon diffusion in $CaCO_3$ calcite. In overall agreement with earlier experimental findings, oxygen diffusion is found to take place possibly by either interstitial or vacancy mechanisms depending on the thermodynamic conditions. Contrary to almost isotropic interstitial diffusion, the vacancy mechanism strongly favors oxygen jumps within (111) planes characteristic of the $CaCO_3$ layered structure, with significant less-than-unity correlation factors. Our simulations show that such mechanisms cannot be applied to carbon, and complex point defects may be required to explain the diffusion of this element. While stability arguments indicate that vacancy complexes formed with CO or CO_3 missing groups may be efficient candidates to convey C diffusion, no low-energy migration path could be identified for these complexes. Focusing on the mostly stable CO vacancy complex and using generic values for unknown migration energies, kinetic Monte Carlo simulations show that this complex mechanism may be responsible for C diffusion roughly 2 orders of magnitude above its oxygen counterpart.

1. INTRODUCTION

Although an apparently well-known textbook case, the $CaO + CO_2 \leftrightarrow CaCO_3$ (de)carbonation process still offers many unknown aspects, in particular as regards the factors controlling its reaction rate; however, this issue has become of high importance in the current context of wide-scale CO_2 handling. While much knowledge on the mechanisms underlying the above reaction has remained essentially empirical for long, currently available experimental as well as theoretical methods of investigations now provide remarkable opportunities to clarify these mechanisms, and special efforts in this direction have been carried out in the last few years. Atomic- scale ab initio simulations were employed to explore such phenomena as (i) CO_2 adsorption[1] on CaO and (ii) $CaCO_3$ nucleation[2] within CaO surfaces. In particular, by demonstrating that nucleation is highly dependent on the type of surface and strongly favored in the presence of (111) indices, the study of ref 2 offered a possibility of interpretation for the noticeable decay of the carbonation rate that occurs during the gradual aging of the CaO substrate induced by the succession of carbonation/calcination cycles. The same issues related to (de)carbonation kinetics were also tackled through experimental works[3,4] relying on state-of-the-art in situ X-ray measurements. By analyzing $CaCO_3$ calcination, the authors concluded that, in contrast with the aforementioned simulation results, no surface selectivity of the reaction could be detected in their experiments. In spite of their somewhat

diverging conclusions, these recent works illustrate, in a case important in practice, the wide interest of confronting experiments and theoretical approaches to elucidate the underlying mechanisms of kinetic processes. They also emphasize that atomic-scale simulations are indeed efficient tools to predict, or at least to suggest, inedited mechanisms, as well as to help unravel intricate situations.

In general, a process such as CaO carbonation may be quite complex as it involves many elemental steps, the overall reaction rate being dictated by the slowest one, the so-called "reaction-limiting step", which itself can be modified as the reaction progresses. In its final stage, namely, when a sufficient carbonate layer has been formed around the CaO grain, it is reasonable to suppose that the reaction rate is controlled by the diffusion of CO_2 through the layer, which may occur through either the bulk or the grain boundaries. In this context, bulk diffusion in calcite itself remains poorly understood, whereas a better understanding of C and O diffusion is desirable, especially as help to infer the behavior of the CO_2 molecule within the compound. Few experimental works have been performed on this issue. However, these works are quite complementary since they tackle either equilibrium diffusion in calcite or nonequilibrium matter transport in the calcite layer growing during the carbonation process. These studies therefore provide a rather good insight into several possible mechanisms underlying diffusion in $CaCO_3$. In a work 5 published in 2004, Labotka et al. performed detailed investigations, by means of the secondary-ion mass spectrometry (SIMS) technique, of C and O diffusion in calcite, between 600 and 800°C in a pressure range from 0.1 to 200 MPa of pure CO_2. They concluded that the oxygen diffusion coefficient remains almost constant over the whole pressure range, whereas increasing the pressure entails a decrease of C diffusion by approximately 2 orders of magnitude. From the identical C and O diffusion coefficients at low pressure, the authors concluded that these thermodynamic conditions should correspond to a regime of joint C and O diffusion through carbonate (CO_3^{2-}) anions. However, the pressure range explored in this work was much higher than usually selected in practical processes for carbonation, and a better understanding of these processes requires complementary investigations at lower pressures. More recently, 6 Sun et al. tackled the issue of non-equilibrium ionic diffusion within the growing calcite layer. Using inert marker experiments, they were able to identify two opposite O^{2-} and CO_3^{2-} anionic diffusion fluxes, respectively, associated with outward (i.e., from the CaO|CaCO3 to the $CaCO_3$|gas interface) and inward currents. On the basis of their observations, these authors confirmed a mechanism, previously proposed[7] in 1983 and commonly admitted, for matter transport through the growing calcite layer, namely, (i) the reaction of O^{2-} ions with CO_2 molecules at the external interface to form carbonate ions, together with (ii) the reaction of the latter ions with Ca^{2+} ions at the inner interface to form $CaCO_3$. It would be interesting to investigate the consequences of this proposed mechanism on the overall kinetics, as obtained from macroscopic simulations or from measurements. The study of ref 6 was however essentially qualitative, with no attempt to measure diffusion coefficients. On the whole, both works suggest that diffusion in $CaCO_3$ may, at least partly, involve carbonate groups allowing both C and O transport and hence two-dimensional (2D) diffusion constrained within the (111) planes of the compound.

Complementary to these experimental results, theoretical investigations of diffusion in calcite would be helpful, but elucidating these intricate issues from atomic-scale simulations implies sufficient knowledge of the properties of point defects (PDs) in $CaCO_3$ since these properties are directly connected with the CO_2 behavior in the compound. Only few atomic-scale studies on calcite[8–12] were concerned with PDs, which were moreover focused on specific kinds of PDs, for example, Ca vacancies. In particular, no results were provided on many other cases, possibly important for

carbonation, such as interstitial defects and various types (C, O, CO_2, etc.) of vacancies. To address these drawbacks, an extended ab initio study of PDs in $CaCO_3$ was performed recently,[13] with thorough investigation of the properties of all types (Ca, C, and O) of elemental defects, including vacancies, antisites, and interstitials. It should however be noted that the analysis of ref 13 was performed under specific thermodynamic conditions, through a particular choice of the carbon and oxygen chemical potentials. Therefore, this previous work clearly urged further improvements to account for the influence of various thermodynamic conditions on C and O diffusion in calcite. A first task of the present work will be to achieve these improvements.

Once settled, these firmer thermodynamic grounds will then offer a sound basis for our atomic-scale study of the diffusion properties of C and O in calcite, the main task of the present work. In particular, through a comparison between the interstitial and vacancy mechanisms, our study will provide a detailed picture of oxygen diffusion. Surprisingly, it will also show that oxygen and carbon have very different behaviors. From the latter feature, an impossibility will arise to apply the same kind of diffusion mechanisms for both species; hence, there is a requirement to investigate the role of complex point defects (CPDs) in $CaCO_3$. Indeed, a similar idea had already stemmed from previous results,[13] pointing out CO_2 vacancies as especially stable CPDs. However, the latter conclusions from ref 13 were preliminary, and the last task of the present work will also be devoted to a detailed inspection of CPDs in calcite, with focus on possible connections between CPDs and joint C + O diffusion in the compound.

The layered structure of $CaCO_3$ quite naturally points out the special role of (111) planes, which suggests a classification of CPDs, according to their belonging to a single (111) plane. Both types of CPDs will therefore be noted -either intra(111) or inter(111) - throughout, and special interest will be devoted to intra(111) CPDs. The latter type of CPDs corresponds to a focus on planar diffusion of CPDs, an approximation that seems reasonable due to the layered crystal structure of $CaCO_3$. Moreover, (111) planes are formed of CO_3 groups, which justifies a secondary classification within intra(111) CPDs, according to their belonging to a single CO_3 group, namely, with two subtypes, noted intra(CO_3) and inter(CO_3). Considering specifically vacancy CPDs, these geometrical classifications will then have to be combined with the various chemical types of CPDs (e.g., CO, CO_2, etc. and vacancy CPDs).

To sum up, the present work is dedicated to an ab initio-based atomic-scale investigation of the diffusion properties of C and O in bulk $CaCO_3$ calcite as a function of the thermodynamic conditions. After introducing the methodological background, the results will be presented, namely, (i) important considerations to settle the thermodynamic basis of the study, (ii) a detailed analysis of the interstitial and vacancy mechanisms, and (iii) the role of vacancy CPDs. The implications of our results in the framework of CaO carbonation by CO_2 will then be discussed.

2. METHODS

First-Principles Calculations. The ab initio calculations were performed using the density functional theory (DFT) as implemented in Vienna Ab initio Simulation Package (VASP) software,[14,15] via the projector-augmented wave framework[16] and the generalized gradient approximation with the Perdew−Burke−Ernzerhof (PBE) form of the exchange–correlation functional.[17] A Gaussian smearing was used, together with a 4x4x4 Monkhorst−Pack k-point mesh and a cutoff energy of 600 eV for the

plane wave basis. All static T = 0 K calculations included relaxations of the atomic positions as well as optimizations of the system size and shape around the PDs.

To obtain the migration profiles for elemental defects, the nudged elastic band (NEB) method was employed as implemented in VASP, using 80-atom systems (containing 2×2×2 $Ca_2C_2O_6$ unit cells) with nine intermediate images and the climbing image technique. In addition, since CPDs have larger volumes than elemental PDs, the influence on their properties of increasing the system size was investigated thoroughly by considering also 270-atom supercells built on 3x3x3 $Ca_2C_2O_6$ unit cells. Finally, it should be mentioned that all of our NEB calculations were performed assuming jump pro fi les for neutral defects, whereas the initial and fi nal states of an atomic transition need not have the same charge level, this condition being a priori fulfilled only in specific cases of symmetric jumps. On the whole, such a "dynamic" effect of charges on migration profiles is still currently a widely open issue, far beyond the scope of the present work.

Modeling of Point Defects and Diffusion. The independent-point-defect approximation (IPDA) offers a convenient way to study point defects and related properties (thermodynamics, diffusion, etc.) in ordered compounds around stoichiometry. Since the IPDA has already been described in its general form[18] and applied[13] to $CaCO_3$, we merely recall here that this approach relies on the determination of grand canonical (GC) energies defined, for a PD of type p and charge q , as

$$E_{GC}(p,q) = E_{PD}(p,q) - E_{perf} \quad (1)$$

where E_{PD} and E_{perf} are, respectively, the total energies of defected and perfect systems of the same size. These energies explicitly depend on the (integer) state of charge of the defected supercells. It should be noted that using charged supercells in ab initio calculations raises intricate issues related to the reference of the electrostatic potential, which may become critical when investigating semiconductor junctions or pressure effects.[19] In our case, preliminary tests on $CaCO_3$ (Supporting Information) indicated that this may induce uncertainties on formation energies below a few tenths of electronvolts, which should not lead to questioning our conclusions about the dominant defects as function of chemical potentials. In this context, since our main purpose in this work was to propose a sufficiently overall description of diffusion for oxygen and carbon (i.e., those species relevant for CO_2 absorption) in calcite, the above issue about corrections to formation energies was not investigated further. It should be appropriately studied as the subject of separate future investigations to reach a more refined picture of the defect and diffusion properties in calcite. From these ab initio input data, the various quantities of PDs are then simply given by

$$x(p,q) = exp\left[-E_f(p,q)/kT\right] \quad (2)$$

with E_f being the formation energy of the PD

$$E_f(p,q) = E_{GC}(p,q) + \delta\mu(p) + q\mu_e \quad (3)$$

where μ_e is the electronic chemical potential, monitoring the global charge of the defected system. $\delta\mu(p)$ is a defect-dependent term involving the elemental chemical potentials: $\delta\mu(p)=+\mu(A)$ for a vacancy (V_A) on an A sublattice, $\delta\mu(p)=\mu(A)-\mu(B)$ for a B antisite atom (B_A) located on an A sublattice, and $\delta\mu(p)=-\mu(A)$ for an A atom (A_{int}) on an interstitial sublattice. The IPDA lends itself to various levels of refinements, for example, by taking into account local defect-induced vibration

contributions to PD energies,[20] and more importantly for the present work, the IPDA formalism offers a convenient point-defect background for diffusion studies[21] and can also quite straightforwardly be extended to charged CPDs.

In addition, it is worth recalling that most previous works on charged PDs, devoted to semiconductors in which global charges do exist (i.e., not to be confused with the local charges around PDs, handled in the present work), investigated explicitly the influence of the electron chemical potential since the global charge is monitored by the latter quantity. The present approach is however different: although various charge states of PDs are also investigated, we consider only globally neutral $CaCO_3$. Therefore, all elemental (i.e., Ca, C, O) chemical potentials being first determined from solid/solid and solid/gas equilibria, the electron chemical potential is then obtained via eq 1 from the global neutrality condition.

Quite generally, the equilibrium diffusion tensor for a given atomic chemical species i reads

$$D_i^{\alpha\beta}{}_{t\to\infty} = lim\,\langle\frac{\delta X_i^{\alpha}(t)\delta X_i^{\beta}(t)}{2t}\rangle \quad (4)$$

where $\delta X_i^{\alpha}(t)$ is the displacement along direction α of a given atom of type i , the average ⟨⟩ being performed on a large population of such atoms. To investigate the diffusion properties of C and O, we will mainly focus on the interstitial and vacancy mechanisms. From this general expression, the diffusion tensor of O for the interstitial mechanism can then be expressed as

$$D_{O(int)}^{\alpha\beta} = \frac{1}{2} f_{O(int)}^{\alpha\beta} \sum_{s,v} \Gamma_{O(int)}^{(s,v)} \delta x^{\alpha}(s,v)\delta x^{\beta}(s,v) \quad (5)$$

with $f_{O(int)}^{\alpha\beta}$ being the tensorial correlation factor for the given mechanism and species. The index s labels the interstitial 6d sites in the $Ca_2C_2O_6$ unit cell (space group $R\bar{3}c$ no. 167; the atomic positions after full structural optimization are provided in Table S1 of the Supporting Information), and v distinguishes between the various jumps possible from each site s. The atomic jump frequencies are given by

$$\Gamma_{O(int)}^{(s,v)} = \frac{c_{O(int)}}{p_O} \gamma_{O(int)}^{(s,v)} \quad (6)$$

where

$$\gamma_{O(int)}^{(s,v)} = \mathrm{f}_{a,O(int)}^{(s,v)} exp\left[-\mathrm{E}_{m,O(int)}^{(s,v)}/kT\right] \quad (7)$$

$\mathrm{F}_{a,O(int)}^{(s,v)}$ and $\mathrm{f}_{m,O(int)}^{(s,v)}$ are the attempt frequency and migration energy for jump (s,v) of interstitial oxygen, respectively, and p_O~6 is the number of sites occupied by O in a unit cell of nearly stoichiometric $Ca_2C_2O_6$. The fraction of interstitial O present on the interstitial sites is obtained from the PD formation energy (eq 3) through

$$c_{O(int)} = exp\left[-E_{f,O(int)}/kT\right] \quad (8)$$

Since in the present case, the γ parameters are identical for all 6d ↔ 6d interstitial jumps within a given level of neighborhood, it is convenient to classify the various jumps according to this level. For interstitial jumps in $CaCO_3$, it will appear sufficient to consider the first two levels 1NN and 2NN,

namely, the first- and second-nearest 6d neighbor shells of a given 6d site, which correspond to the fourth and seventh absolute neighbor shells of this site. Finally, it is a well-known fact that the correlation factor for the interstitial mechanism is unity. Therefore, the O diffusion tensor for this mechanism can be reformulated as

$$D_{O(int)}^{\alpha\beta} = \frac{c_{O(int)}}{12}\left[\gamma_{O(int)}^{1NN} S_{1NN}^{\alpha\beta} + \gamma_{O(int)}^{2NN} S_{2NN}^{\alpha\beta}\right] \quad (9)$$

with

$$S_{1NN}^{\alpha\beta} = \sum_s \sum_{v \in 1NN(s)} \delta x^{\alpha}(s,v)\delta x^{\beta}(s,v) \quad (10)$$

The notation $v \in 1NN(s)$ refers to those jumps v reaching the 1NN shell of site s, and $S_{2NN}^{\alpha\beta}$ is given by an analogous expression. While 2NN interstitial jumps produce three-dimensional (3D) diffusion, 1NN jumps only allow for diffusion within the (111) planes. It is noteworthy that due to the absence of correlation for the interstitial mechanism, eq 9 yields a reasonably accurate analytical estimation of the diffusion tensor and will thus be used next.

For the vacancy mechanism, a similar expression can easily be established

$$D_{V(O)}^{\alpha\beta} = f_{V(O)}^{\alpha\beta} \frac{c_{V(O)}}{12} \sum_p \gamma_{V(O)}^{pN_{abs}} S_{pN_{abs}}^{\alpha\beta} \quad (11)$$

where pN_{abs} refers to the p^{th} absolute neighbor shell of jumps on the O sublattice. To avoid possible confusion with interstitials, this notation will be preferred for the vacancy mechanism. For completeness, a set of four levels p ∈ {2,4,5,6}, corresponding to the four shortest jumps between two O sites, will be included in the following study. In general, the correlation factor for a given diffusion mechanism is not unity, and its analytical evaluation is a rather complicated task. Therefore, except in the aforementioned interstitial mechanism, an atomic-scale kinetic Monte Carlo (KMC) simulation approach was preferred in the present work, relying on direct evaluation of eq 4 and comparison with analytical expressions such as eq 11. For these KMC simulations, a standard residence-time algorithm was used. In this approach, which offers the advantage of including naturally the correlation effects, the atomic diffusion is mediated by the presence of an isolated PD of a given type in the simulation supercell, the size of which directly determines the PD concentration in the compound and thus the magnitude of the atomic diffusion tensor. Note that the latter scales linearly with the PD concentration, as can be easily checked. In the present work, two types of KMC simulations were performed, in either three or two dimensions. Three-dimensional simulations were applied to the previously described oxygen vacancy mechanism, which yielded the corresponding correlation factor. Such an accurate evaluation of $D_{V(O)}^{\alpha\beta}$ was required to allow comparison between the interstitial and vacancy mechanisms.

Conversely, 2D simulations were concerned with diffusion mediated by vacancy complex PDs since such CPDs may play an important role in $CaCO_3$. In particular, many previous works refer to the role of the CO_3^{2-} carbonate ion, which might move through $V(CO_3^{2-})$ vacancy CPDs. From geometric arguments related to the layered structure of calcite, it is highly probable that these movements occur in (111) planes, which justifies the use of 2D KMC simulations for such vacancy CPDs. As a main feature, vacancy CPD-based mechanisms allow a joint diffusion of C and O: in the case of $V(CO_3^{2-})$, the relation is simply $D_{O[V(CO3)]} = D_{C[V(CO3)]}$ (omitting the charge for brevity, and the notation $O[V(CO_3)]$

referring to O diffusion mediated by V(CO_3) CPDs), since the analogy is evident with a simple vacancy mechanism. Moreover, our study will suggest that other types of vacancy CPDs can be considered for which the previous equality no longer holds. Therefore, 2D KMC simulations offer a convenient way to investigate issues related to vacancy CPD-mediated joint C and O diffusion. Figure 1 displays the 3D and 2D unit cells of $CaCO_3$ used for our KMC simulations, together with the orientation of the orthonormal basis ($\mathbf{u}_1$,$\mathbf{u}_2$,$\mathbf{u}_3$) in which all diffusion tensors were expressed. Figure 1 shows that the orientation of the KMC system with respect to this basis is the same for 2D and 3D simulations.

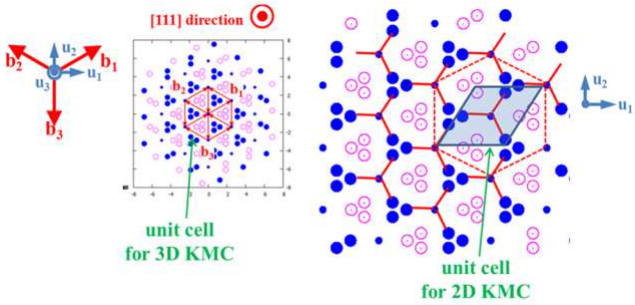

Figure 1. Crystal structure of $CaCO_3$ calcite, projected onto the (111) plane, and showing the 3D and 2D unit cells used in kinetic Monte Carlo simulations of diffusion. ($\mathbf{b}_1$,$\mathbf{b}_2$,$\mathbf{b}_3$) are the lattice vectors of the rhombohedral primitive cell, and ($\mathbf{u}_1$,$\mathbf{u}_2$,$\mathbf{u}_3$) is the orthonormal basis used for the numerical evaluations of all diffusion tensors.

3. RESULTS

Thermodynamic Conditions Relevant for C and O Diffusion in Calcite. To elucidate the mechanisms under-lying the transport of C and O through the $CaCO_3$ layer, it is required to have as accurate as possible a description of the thermodynamic conditions to which the growing carbonate layer is subjected. Handling this topic with sufficient detail is required to settle our subsequent analysis of diffusion properties on a firm ground. To this aim, it is supposed isothermal conditions with T = 800 K (a typical working temperature in experiments) throughout this work; the chemical potentials μ(C) and μ(O) of the C and O species are the central quantities since their spatial pro fi les control the matter transport phenomena across the carbonate layer. For our purpose, it will be equivalent and more convenient to characterize the quantities μ(O) and A=μ(C)+2μ(O). It is essential to keep in mind that overall consistency requires that the same ab initio energetics be employed for the (μ(O); A) determination and for the diffusion study as done in the present work. In this context, both interfaces delimiting the calcite layer have an important role since they induce a priori distinct constraints on the chemical potentials.

Near the internal ("int") interface, namely, for μ_{int}(C) and μ_{int}(O), the A quantity is relevant, since using free energies G, the CaO|$CaCO_3$ equilibrium entails that $G(CaCO_3)-G(CaO)=\mu_{int}(C)+2\mu_{int}(O)=A_{int}$. In a previous work[13] using the same ab initio framework, A_{int} was evaluated simply via the T=0 K energies for both compounds, that is, $E(CaCO_3)=-37.45$ eV and $E(CaO)=-12.88$ eV; hence, A_{int}(0 K)=−24.57 eV, indicating that the [−25; −24 eV] range should be characteristic of A near the internal interface. However, the accuracy of this earlier A_{int} evaluation[13] has to be discussed with respect to possible $CaCO_3$ off-stoichiometry as well as temperature effects. First, as regards some possible $CaCO_3$ off-stoichiometry, the IPDA framework described in the previous section conveniently allows one to investigate this possibility (as displayed in Figure S1a of the Supporting Information). It shows that this issue should not be critical since the stoichiometry of the compound is almost perfect in a

wide range of A and μ(O) values, at least for temperatures of interest. Second, as concerns temperature effects, it is important to investigate whether the A_{int} variable may be modified by atomic vibrations in the CaO and $CaCO_3$ crystalline compounds. To this aim, ab initio calculations (see Figure S1b in the Supporting Information) confirm that the effect of atomic vibrations remains negligibly small. On the whole, our results demonstrate that whatever the temperature and $CaCO_3$ stoichiometry, the [−25; −24 eV] range can be reasonably regarded as representative of A values near the internal interface. Conversely, while these considerations allow selecting a plausible range for A , the question of choosing μ(O) appears to be much more intricate, especially near the internal interface, since this parameter is not settled there by some well-defined equilibrium. In our previous investigations,[13] we had supposed, in a simplified view, that $\mu_{int}(O) = \mu_{ext}(O) = \mu_{gas}(O_2)/2$, but this is probably not representative of the situation at the internal interface, and it will thus be preferable to keep μ(O) as a control parameter in the present diffusion study.

The same issue arises at the external interface, in contact with a gas phase either made of pure CO_2 or containing this gas within a gaseous mixture including an inert gas. Experiments are usually carried out under a fixed CO_2 partial pressure, which allows one to control the quantity $A_{ext} = \mu_{ext}(C) + 2\mu_{ext}(O)$. Conversely, it should be noted that these experimental conditions do not allow one to control separately $\mu_{ext}(C)$ and $\mu_{ext}(O)$, since to guarantee such separate controls, the partial pressure of the O_2 gas should also be fixed. This is usually not done in practice, and it is commonly admitted that O_2 is present only at residual partial pressures. In our previous work[13] on PDs in $CaCO_3$, we had therefore supposed the existence of a small O_2 pressure of 100 Pa, and applying an ab initio-based statistical physics analysis to the O_2 phase, supposed to be a perfect gas, we had been able to show that the O "external" chemical potential at 800 K should be $\mu_{ext}(O) \sim -5$ eV in the selected ab initio energy framework. Since the CO_2 partial pressure is also rather low (a few kPa) in many experiments, a similar treatment for the perfect CO_2 gas phase allowed estimating A_{ext} in the [−25; −24 eV] range, from which the value $\mu_{ext}(C) \sim -15$ eV was selected at 800 K. The latter choice of $\mu_{ext}(C)$ and $\mu_{ext}(O)$ values was referred to as "O_2+CO_2 conditions" in ref 13, since this set of chemical potentials was obtained through a control of both the O_2 and CO_2 gases and was used to study the PD properties of $CaCO_3$. Although somewhat arbitrary for the O_2 gas, such a simplifying choice was made compulsory by the aim of ref 13 to keep tractability when performing a global survey of all types of charged PDs in the compound. In the present work, the purpose is different: mainly the C and O vacancy and interstitial defects will be considered since these PDs are expected to be mostly relevant for diffusion. As regards the thermodynamic conditions near the external interface, it should also be noticed that the effect of much higher CO_2 pressures, for example, up to 2 kbar as in ref 5, may lead to a significant increase of A_{ext}. Indeed, following a thermostatistics approach similar to that mentioned in ref 13 to obtain $\mu_{gas}(CO_2)=A_{ext}$ suggests that $A_{ext} \in$ [−24; −23 eV] would be more realistic for such pressures. On the whole, this analysis therefore indicates that for the ab initio energetics chosen in our work, the [−25; −23 eV] range for A can be used safely near both the internal and external interfaces.

Using the full set of energy data for charged PDs described in ref 13 (with 2×2×2 $Ca_2C_2O_6$ defected supercells), the effect of A and μ(O) on the C and O point defects in $CaCO_3$ was calculated as a function of μ(O) for various A values. Figure 2 displays the corresponding PD formation energies at 800 K. The hatched zones denote the limits of the stability domain of the compound, as obtained from the PD modeling, to ensure that off-stoichiometry remains reasonably low. In particular, crossing these limits abruptly entails an unrealistic behavior of the model $CaCO_3$, related to a

formation energy becoming vanishingly small for some PDs and hence a diverging behavior for the atomic fractions (as depicted in Figure S1a). Thus, characterized by almost perfect stoichiometry at 800 K, the stability domain of calcite appears to be located between the bounds μ(O) ∼ − 9 and − 5 eV, with some small variations of these bounds depending on the A value. As regards the C and O defects, Figure 2 shows that μ(O) has a drastic effect on their stability. For interstitial C, although our previous study[13] suggested that this defect may decay into a complex PD under thermal agitation, it was included in our calculations for completeness, but Figure 2 clearly confirms that it should be ruled out due to its high formation energy >4 eV whatever the thermodynamic conditions. The other C defect, namely, the carbon vacancy V(C), also appears too energetic to play a significant role in diffusion. At this point of our study, it is worth noting that these considerations on PDs unexpectedly lead to discarding the interstitial as well as the vacancy diffusion mechanisms for C, which raises an important issue about the existence of alternative mechanisms possibly active for this element. Such mechanisms may involve vacancy complex PDs and in particular (but not only) the $V(CO_3)$ complex moving in (111) planes. This issue will be dealt with further later.

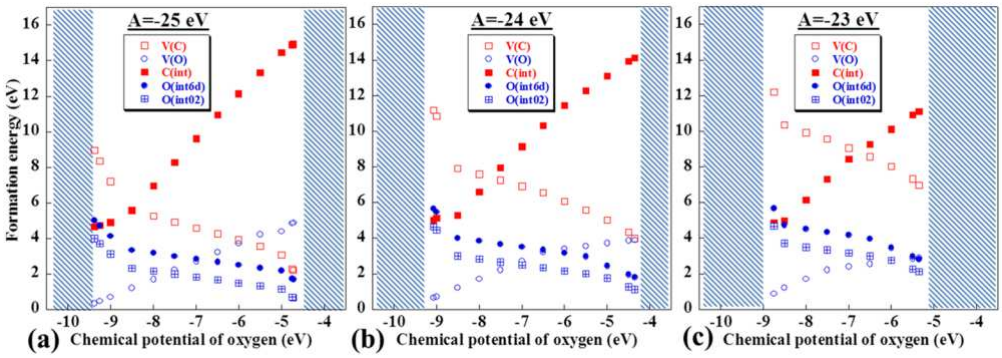

Figure 2. Effect of oxygen chemical potential on the T = 800 K properties of C and O point defects in $CaCO_3$, either of vacancy or of interstitial type, for various values of A=μ(C)+2μ(O): (a) A=−25 eV, (b) A=−24 eV, (c) A=−23 eV, as obtained from ab initio calculations. For interstitial O, two configurations are considered (see text for details).

For O defects, the situation is much clearer since the limits of the stability domain correspond to a strong enhancement of these defects, either V(O) for lower values of μ(O) ∼ −9 eV or O(int) for higher values μ(O) ∼ − 5 eV. From our previous considerations, the upper limit for μ(O) probably matches the thermodynamic conditions at the external interface, which points out O(int) as the probable main PD in the outer part of the growing layer. Conversely, we have already mentioned that the μ(O) conditions near the internal interface are much more di ffi cult to be made precise. At this stage, it would thus be irrelevant to rule out a priori the possibility of a strongly negative μ (O) near the internal interface, a scenario entailing a change of dominant PD and hence a change in the diffusion mechanism of oxygen across the calcite layer. Finally, a remarkable feature related to interstitial oxygen has to be emphasized: while the usual Wyckoff 6d position was employed initially for both C and O interstitials, another interstitial configuration, noted “int02” and discussed further below, had to be introduced for O. The enhanced stability of the int02 configuration further confi rms O(int) as the dominant O defect in the outer part of the calcite layer.

Diffusion Mechanisms for Oxygen. *Interstitial Mechanism.* As recalled previously, the migration energies (E_m parameters in eq 7), being the main quantities required to investigate diffusion

mechanisms, are usually extracted from energy pro fi les obtained by the NEB method. These profiles for the 1NN and 2NN jumps of oxygen are displayed in Figure 3, and Table 1 lists the corresponding E_m values. As a first remarkable feature, these pro fi les display a new, unexpected "interstitial" configuration, notably more stable (by ∼0.7 eV) than the expected 6d Wyckoff position. Due to the identification of this new int02 configuration, it became necessary to revisit the PD properties (as displayed in Figure 2), since, in general, the coupling between the various types of defects in the IPDA formalism implies that a significant change in the energetics of a single PD may affect the whole PD structure. We however checked that this is not the case for $CaCO_3$ since only the amount of O(int) is affected by the int6d → int02 switch. Nevertheless, Figure 2 shows that especially for lower A values, the int02 configuration induces a significant downward shift of O(int) formation energies. This confirms the high stability of interstitial oxygen for μ(O) ∼−5 eV, which should reflect the thermodynamic conditions near the carbonate − gas interface. This new interstitial configuration is probably related to the intricate crystallography of $CaCO_3$, which emphasizes that studying such low-symmetry compounds from atomic-scale simulations is still currently not a straightforward task. As a second remarkable feature of O(int) jumps, the 2NN is much more favorable (by ∼0.8 eV) than the 1NN one, and the diffusion properties of interstitial oxygen thus cannot be deduced from a simple first-nearest neighbor analysis. It will be shown next that including the 2NN jumps leads to satisfactory predictions on the O(int) diffusion tensor. For the latter reason, O(int) jumps beyond 2NN were not investigated, all the more as they should be rather unrealistic due to their large jump distances (>4 Å).

Most diffusion studies are built solely from migration energies, assuming for the various attempt frequencies a single generic value, usually chosen of the same order as phonon frequencies (typically ∼10 THz). However, recent investigations[20] have demonstrated that this may be a severe hypothesis, at least in metallic systems, since ab initio calculations in metallic ordered compounds revealed the existence of a wider panel of frequencies. Therefore, it is instructive to improve our knowledge of attempt frequencies in ionic compounds such as $CaCO_3$. To help answer this question, using the approach described in ref 20, we calculated the attempt frequencies for the 1NN and 2NN interstitial O jumps, and these quantities are displayed in parentheses in Table 1. Interestingly, while the 2NN frequency has a rather common value (∼15 THz), the frequency for the 1NN jump is somewhat higher (∼53 THz), both values being in reverse order with respect to the migration energies. However, this limited jump-sensitivity of attempt frequencies should not significantly modify the trends for diffusion investigated here. The diffusion tensor at 800 K resulting from these data through eq 9 is displayed in Figure 4, as a function of the oxygen chemical potential and for A=−24 or −25 eV. The profiles, which reflect the O(int) formation energies (Figure 2), indicate that the interstitial mechanism may be active only for higher values of μ(O). In this μ(O) range, depending on A, the diffusion coefficient may potentially exceed 10−14 cm^2/s, in good agreement with experiments.[5] Although the latter were performed at a somewhat higher temperature (1073 K) and under high pressures (1−2000 bar), a pressure increase should be translated into a higher A value, which according to Figure 4 entails a lowering of diffusion. Since the latter effect may itself be compensated by a temperature increase from 800 to 1073K, our results appear to confirm these previous experiments as regards the efficiency of the interstitial mechanism for O diffusion in calcite. As explained in the previous section, our conclusions on oxygen diffusion are more reliable for μ(O) representative of the external interface, which is consistent with the fact that the SIMS technique used in these experiments primarily captured the oxygen profile near this interface. It should also be

noted that the 2NN jumps are essential to reach an agreement with the experiments of ref 5. Moreover, our calculations reveal for the interstitial mechanism a significant anisotropy, directly related to the anisotropy of the S tensor (eq 10): the diffusion within the (111) planes lies about 1 order of magnitude below that along the direction perpendicular to these planes. Although not altering qualitatively the good efficiency of the mechanism, this feature is not to be overlooked as it might be connected with a dependence of diffusion upon the texture of crystallites in calcite. In particular, if this texture evolves during the carbonation−decarbonation cycles, this may help explain the slowdown of the carbonation kinetics usually noted in practice.[3]

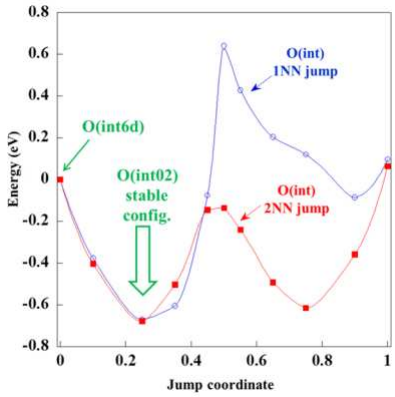

Figure 3. Energy pro fi les for first- (1NN) and second-nearest-neighbor (2NN) jumps of interstitial oxygen in CaCO3, obtained from ab initio calculations with the NEB technique. The pro fi les evidence the int02 configuration, more stable than the 6d Wyckoff position expected from crystallographic arguments. As for the 1NN pro fi le, its strong slope on the left side around the maximum is simply due to the presence of the 02 position, which implies a dissymmetrical repartition of the NEB images on both sides of the maximum. In spite of this dissymmetry, the energy barrier for this jump is reasonably provided by the current profile.

Table 1. Migration Energies (eV) for O Diffusion in CaCO3 As Obtained from ab Initio Atomic-Scale Simulations[a]

	1NN		2NN	
O(int)	1.33 (53)		0.55 (16)	
	$2N_{abs}$	$4N_{abs}$	$5N_{abs}$	$6N_{abs}$
V(O)	0.99	1.31	0.49	1.51

[a]For the interstitial mechanism, the energies are referred to the int02 stable con fi guration identified (Figure 3). The values in parentheses are the corresponding attempt frequencies (THz), as calculated from the transition rate theory using both the PD and saddle-point phonon spectra.

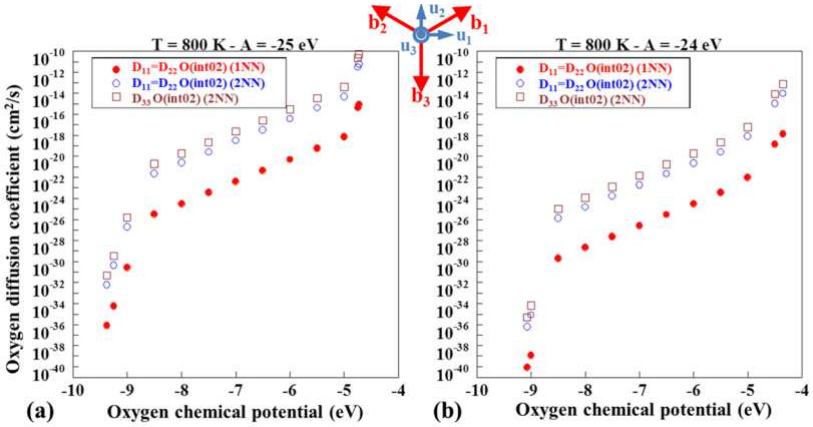

Figure 4. Influence of oxygen chemical potential and (a) A=−25 eV, (b) A=−24 eV on the T=800 K diffusion tensor of interstitial oxygen in $CaCO_3$, from eq 9 and the ab initio-based data of Table 1, and considering either 1NN or 2NN jumps. Note that in the case of 1NN jumps, the tensor is two-dimensional (diffusion is confined in (111) planes).

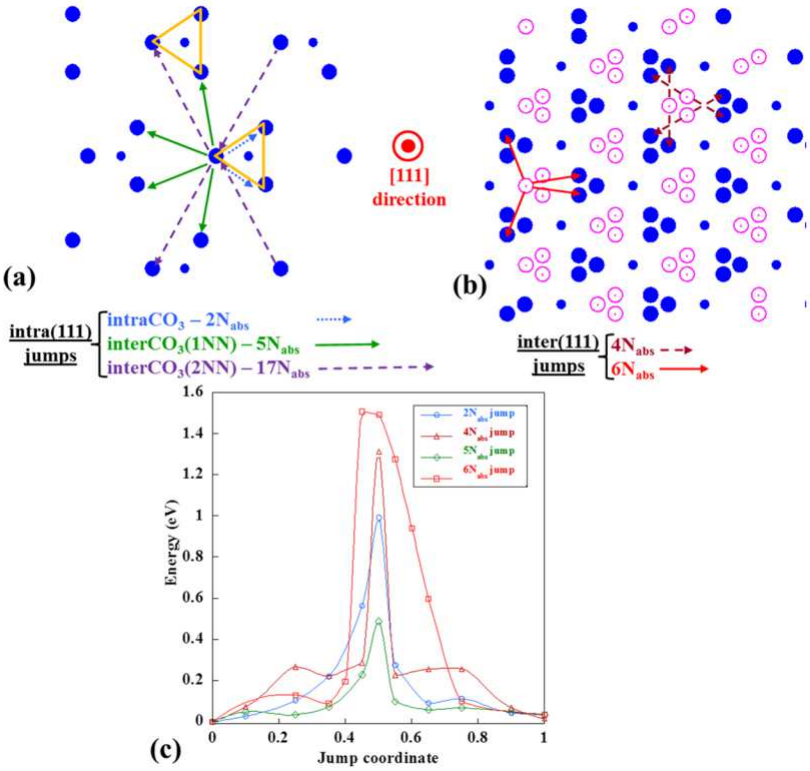

Figure 5. Vacancy mechanism for O diffusion in $CaCO_3$: fi gures (a) and (b) depict the various jumps considered, that is, (a) intra(111) jumps in a single (111) plane; and (b) inter(111) jumps between different (111) planes (with full projection of all planes on the figure); figure (c) displays the corresponding migration profiles obtained from ab initio calculations with the NEB technique.

Vacancy Mechanism. Figure 5a,b depicts the various jumps considered for the O vacancy, these jumps being either contained within a single (111) plane (i.e., intra(111) jumps, Figure 5a, hence 2D diffusion) or fully three-dimensional (i.e., inter(111) jumps, Figure 5b). Only the two shortest

intra(111) jumps (2N abs and 5N abs absolute neighborhoods) were studied owing to the excessive range of the next intra(111) jump ($17N_{abs}$) making it unrealistic. Contrary to the 5N abs jump connecting two distinct CO_3 groups (hence referred to as "interCO_3"), the 2N abs jump merely amounts to an internal movement of the O vacancy within the CO_3 group ("intraCO_3" jump) and thus is not diffusive by itself. However, it may have an influence on the full vacancy mechanism and will thus be included in the analysis, in conjunction with the other types of vacancy jumps. As for inter(111) jumps, while $6N_{abs}$ jumps are responsible for fully 3D diffusion, it should be noted (Figure 5b) that the pair of $4N_{abs}$ jumps from a given O site only connects two neighboring sites aligned with the initial site. As a consequence, allowing only $4N_{abs}$ jumps leads to "channel diffusion" due to the confinement of the V(O) defect within a line, which leads to erroneous diffusion properties, as confirmed by the KMC simulations presented below. Therefore, similar to the $2N_{abs}$ case, the $4N_{abs}$ jumps should only be included in conjunction with other types of vacancy jumps.

The migration profiles for these various O vacancy jumps are displayed in Figure 5c, and the migration energies are listed in Table 1. Although somewhat higher than for the interstitial case, the O vacancy migration energies have moderate values, suggesting a possible efficiency of the V(O) mechanism. The $6N_{abs}$ jump, the only one with fully 3D diffusive character, is somewhat less favorable than other vacancy jumps. Although not as justified as in the interstitial case due to less-than-unity correlation, it is instructive to perform first an analytical evaluation of the V(O)-mediated diffusion tensor of oxygen, via eq 11 and neglecting the correlation factors. Figure 6 displays the result of this evaluation for each pN_{abs} neighborhood separately. While the main contribution appears to stem from planar diffusion ($5N_{abs}$ jumps), 3D jumps display some anisotropy, with preference for diffusion along the [111] direction. Moreover, reflecting the PD properties, the V(O)-mediated diffusion of oxygen is mainly active for strongly negative values of the oxygen chemical potential. In this μ(O) range, due to the high stability of the V(O) defect, it may reach the same level of efficiency as interstitial diffusion.

To go one step further with the O vacancy mechanism, these conclusions drawn from these analytical diffusion models have to be confronted with the predictions of KMC simulations, the latter being able to account for correlation effects. The relevant simulations were carried out including the four types of V(O) jumps mentioned above, using two sizes for the KMC system, namely, either 3×3×3 or 10×10×10 $Ca_2C_2O_6$ unit cells, for better check of the results. Generic values (10 THz) of attempt frequencies were used here since our previous study of interstitial jumps indicated that these parameters are not expected to modify the order of magnitude of diffusion. Such simulations at 800 K (see Figure S2 in the Supporting Information) confirm the satisfactory convergence of the diffusion tensor (eq 4) during the simulation time, the fluctuations being lowered when increasing the system size. The tensorial correlation factor for V(O) diffusion could be evaluated from eq 11 and is collected in Table 2, for KMC simulations including all types ($2N_{abs}$, $4N_{abs}$, $5N_{abs}$, and $6N_{abs}$) of vacancy jumps ("all jumps" column). The f values for both system sizes are close and lie between 0 and 1 (both features that confirm the validity of our approach) while revealing a strong anisotropy: $f_{11}=f_{22} \ll 1$ in contrast with f_{33}. Also displayed in Table 2 are the results of KMC simulations including only a single type of jump, either $5N_{abs}$ or $6N_{abs}$ (as mentioned previously, similar calculations were found to be irrelevant for non diffusive $2N_{abs}$ and $4N_{abs}$ jumps). Correlation outside (111) planes (i.e., f_{33}) appears to be strongly dependent on the type of jumps selected, which demonstrates the interplay between the various types of jumps. Moreover, correlation being more significant within the (111) planes ($f_{11}=f_{22}<f_{33}$), this effect should therefore lower the anisotropy of the V(O)

mechanism (without correlation, $D_{11}=D_{22}\gg D_{33}$ from Figure 6). Nevertheless, even including correlation effects, the intensity of intra(111) diffusion remains roughly 2 orders of magnitude above that along the [111] direction (Figure S2). This contrasts with interstitial O diffusion, which was predicted to be more favorable along [111]. On the whole, our investigations show that both the interstitial and vacancy mechanisms may potentially be active for oxygen diffusion in $CaCO_3$: the high amounts of PDs, as well as the low energy barriers for PD migration, fulfill the requirements for this phenomenon to occur efficiently. In this context, it is worth emphasizing again that the critical quantity for mechanism selection is probably the oxygen chemical potential at the internal $CaO|CaCO_3$ interface. Specific studies, beyond the scope of this work, would be instructive to elucidate the features monitoring this quantity.

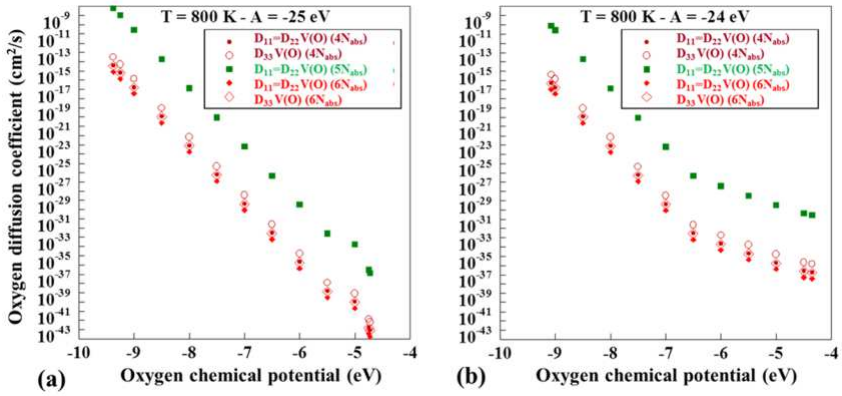

Figure 6. Taking unity for correlation factors, diffusion tensor of oxygen by O vacancy mechanisms at 800 K for various conditions of oxygen chemical potential and (a) A=−25 eV, (b) A=−24 eV. The evaluation was performed analytically, using eq 11 together with the ab initio-based input data of Table 1 and various jump neighborhoods.

Table 2. Correlation Factors (Diagonal Components of Tensor $f^{\alpha\beta}$) for Oxygen Diffusion by the Vacancy Mechanism in $CaCO_3$, from ab Initio-Based KMC Simulations at T=800 K[a]

KMC system size	V(O) fraction	$f_{11}=f_{22}$ (all jumps)	f_{33} (all jumps)	$f_{11}=f_{22}$ ($5N_{abs}$ only)	$f_{11}=f_{22}$ ($6N_{abs}$ only)	f_{33} ($6N_{abs}$ only)
$3\times3\times3$	6.2×10^{-3}	0.26	0.95	0.18	0.27	0.51
$10\times10\times10$	1.7×10^{-4}	0.21	0.94	0.19	0.27	0.47

[a]The size of the KMC system is specified by the number of $Ca_2C_2O_6$ unit cells.

Diffusion of Carbon and Role of Complex Point Defects. *Vacancy Complex Point Defects in Calcite.* Following our purpose, the aim of this section will be to provide for carbon a counterpart of the previous results devoted to oxygen diffusion in $CaCO_3$. However, when tackling this task, a new difficulty arises since the usual mechanisms resting on interstitial and vacancy C point defects, and shown to be efficient for oxygen, have to be ruled out. Indeed, as shown in a previous work using atomic-scale simulations,[13] interstitial C appears to be an unstable PD in $CaCO_3$, spontaneously decaying into a hardly mobile CPD. Moreover, as displayed in Figure 2, the energy cost of the V(C) defect is high, whatever the chemical potential conditions chosen, which suggests that the vacancy mechanism cannot be considered as efficient for C diffusion in calcite. In this framework, the

guidelines used for O diffusion cannot be followed for carbon, and more specific mechanisms, relying on complex PDs, should be introduced. Although the realm of CPDs is much larger than that of simple ones, it seems natural to consider first CPDs consistent with C transport, and to this purpose, CPDs implying C vacancies naturally come to mind. Having characterized previously the roles of isolated vacancies and interstitials, it may seem natural to consider first the possibility of binding between these elemental defects, which corresponds to so-called Frenkel pairs. Ab initio calculations (using 2×2×2 $Ca_2C_2O_6$ supercells) were thus performed on such defects with various charge levels (Figure S3), which pointed out, for O as well as C, a marked trend toward recombination V+int→∅. This trend, visible for neutral and positive defects and possibly connected with the metastability of 6d interstitial sites detected previously, suggests that Frenkel pairs may be irrelevant for O and C diffusion. However, our above results demonstrate that Frenkel defects are not essential in interpreting the levels of O diffusion noted experimentally. Moreover, since they induce a specific correlation between C and O jumps, it is unlikely that these defects may account by themselves for the net 2:1 ratio of O/C diffusion required for the carbonation reaction at the internal interface. In this context, although not fully discarded, the possibility that Frenkel defects may be active for C and O diffusion in calcite was therefore not studied further (leaving such studies for future dedicated works possibly with refined DFT functionals) in favor of other types of complexes detailed below.

The layered crystal structure of $CaCO_3$ leads to focusing on the properties of the CO_3 groups contained within (111) planes and hence the various types of intra(CO_3) vacancy CPDs potentially important for diffusion properties, namely, V(O_2), V(CO), V(CO_2), and V(CO_3). In particular, it seems logical to pay special attention to V(CO_3) since previous studies of diffusion in calcite[5,6] have suggested the likely role of carbonate ions CO_3^{2-} in this process. Moreover, whereas V(O_2) is not related to C diffusion, it will be investigated as well in the following, for the sake of completeness among intra(CO_3) CPDs. When dealing with CPDs, the influence of the size of the system used in ab initio calculations on the E_{PD} and E_{GC} quantities (eq 1) must be carefully taken into account because the volumes affected by CPDs are larger than for elemental defects, which may entail spurious interactions between a CPD and its "images" coming from periodic boundary conditions. To clarify this issue, a comparison (not shown for brevity) of $E_{GC}(q)$ values, obtained for either 2×2x2 or 3×3×3 systems, for the various intra(CO_3) vacancy CPDs under various charge states (between -4 and +4), was carried out. It demonstrated the good agreement between the results obtained for these two sizes of ab initio systems, indicating that the CPD study can safely be pursued using 3×3×3 systems.

The formation energies of charged CPDs were then calculated in the same way as for elemental PDs, using eq 3 with appropriate values of $\delta\mu(p)$ terms (for instance, $\delta\mu = +\mu(C)+2\mu(O)$ for V(CO_2)). As a first step, using chemical potential values $\mu(C)=-15$ eV and $\mu(O)=-5$ eV pointed out previously[13] as roughly representative of the thermodynamic conditions through a calcite growing layer (at least not too far from the external interface), clear trends can thus be noted for intra(CO_3) vacancy CPDs (Figure 7a): (i) whatever its charge, the highly energetic V(O_2) complex has low stability in $CaCO_3$, (ii) conversely, the V(CO) has a surprisingly low formation energy (below $\sim$ 2 eV), with a wide range of stability for charges between − 2 and 0, and (iii) the V(CO_2) and V(CO_3) complexes also have quite low formation energies (though somewhat higher than V(CO)), the neutral (respectively q = +2) state being clearly more favorable for V(CO_2) (resp. V(CO_3)). On the whole, the formation energies obtained in the present work suggest that diffusive properties should be a priori considered for

V(CO), V(CO_2), and V(CO_3), each of these CPDs being possibly consistent with a joint diffusion of carbon and oxygen and allowing atom movements only within (111) planes.

In addition to these intra(CO_3) CPDs, it is useful to consider CPDs of inter(CO_3) type, namely, belonging to a pair of neighboring CO_3 groups, because such CPDs may be intermediate steps for the diffusion of intra(CO_3) CPDs. More precisely, two types of intra(111) diffusion mechanisms involving vacancy CPDs can be considered a priori: either (i) direct CPD jumps between neighboring (CO_3) groups (i.e., a one-step intra(CO_3) → intra(CO_3) sequence), or (ii) jumps involving an intermediate step of "decomposition" of the CPD (i.e., a two-step intra(CO_3) → inter(CO_3) → intra(CO_3) sequence). While the above results demonstrate that intra-(CO_3) CPDs can be easily investigated, several energetically nonequivalent variants are possible for inter(CO_3) CPDs, which strongly raises the level of intricacy. In this context, it is reasonable to focus on inter(CO_3) V(CO) due to its intriguing stability already denoted in intra(CO_3) configurations (Figure 7a). In the inter(CO_3) form, this CPD can adopt four variants, which are depicted in the inset of Figure 7b. Displaying the formation energies of these variants (in the same thermodynamic conditions as in Figure 7a), Figure 7b shows that the energy levels for inter(CO_3) variants are globally high, except for V4, q = +1. Moreover, while at this stage, all CPDs (either intra(CO_3) or inter(CO_3)) considered were of intra(111) type, a similar behavior was obtained for a selected inter(111) jump (full symbols in Figure 7b), which emphasizes the high difficulty of reaching a comprehensive overview of CPD-mediated diffusion in calcite, especially if inter(CO_3) and/or inter(111) configurations are included. Therefore, to maintain tractability in the present work, we stick to intra(CO_3) CPDs and explored for these CPDs the effect of varying the μ(O) and A thermodynamic parameters (Figure 7c,d). As concerns V(O_2), although a narrow domain of μ(O) (low values) is consistent with its stability, this CPD was not considered further for diffusion since it was shown previously (Figure 6) that the elemental O vacancy mechanism is sufficient to account for O diffusion in this range of O chemical potential. Similarly, since the formation energy of V(CO_2), which does not depend on μ(O), remains high whatever the A value, it seems reasonable to rule out this CPD as well. Conversely, our calculations indicate that V(CO) and V(CO_3) must be retained as potentially active CPDs, with vanishingly small formation energies possibly reached for V(CO_3). As already seen for O vacancies and interstitials, the CPD stability appears to be strongly influenced by the thermodynamic conditions, which further raises the issue of understanding how μ(O) is settled in experiments. In a previous work,[13] it was demonstrated that μ(O) can undergo strong variations, depending on the presence of (i) significant (controlled) partial pressure of O_2 gas, (ii) residual (uncontrolled) amounts of O_2 gas, and (iii) other gaseous components such as water vapor. In this context, while stability of V(CO) (higher μ(O), i.e., μ(O)∼−5 eV) should occur only if condition (i) is fulfilled, the stability domain of V(CO_3) ("low μ(O)", i.e., μ(O)∼−9 eV) may be consistent with either condition (ii) or (iii). Therefore, unless the elemental chemical potentials are well-controlled, it may be difficult to determine properly if V(CO) or V(CO_3) is present in experiments. From our formation energy criteria, either CPD may thus be potentially active for diffusion.

Diffusion Properties from Vacancy CPDs. Bearing in mind these results on CPDs, we first explore the diffusive properties of V(CO_3), as sketched in Figure 8a for a jump between two neighboring CO_3 groups. Using 3×3×3 $Ca_2C_2O_6$ systems for NEB calculations, the corresponding energy profile could be obtained (Figure 8b), leading to a migration energy E_m∼5 eV, a value that clearly is too high for V(CO_3) diffusion to be operative in calcite. Due to the somewhat intuitive role of (111) planes, it is surprising that no easy V(CO_3) movement could be evidenced in these planes, all the more since

previous experimental studies of diffusion in calcite did commonly consider matter transport via CO_3^{2-} carbonate ions as an accepted fact. While some deficiency of the DFT exchange − correlation functional used in the present work cannot be disregarded to explain this surprising result, the latter doubtlessly points out that complementary work would be useful to clarify this issue.

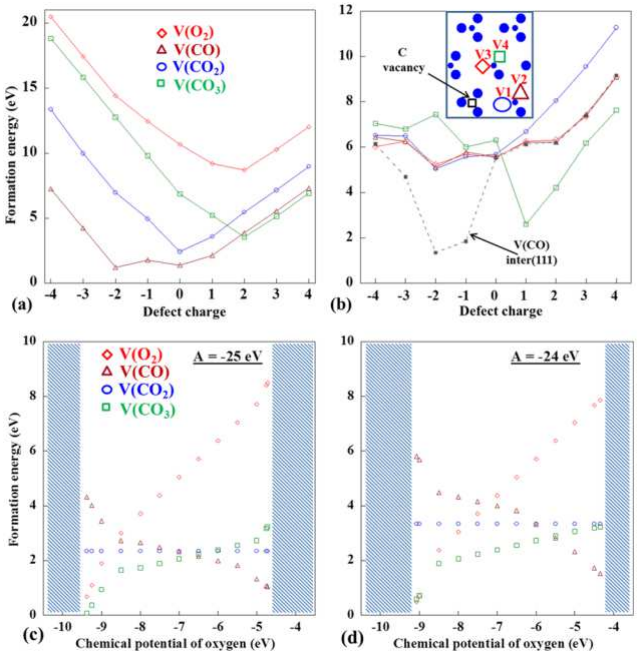

Figure 7. (a) Formation energies of intra(CO_3) charged CPDs in calcite, for chemical potentials μ(C)=−15 eV and μ(O)=−5 eV; (b) same as (a), for inter(CO_3) CPDs; (c,d) influence of thermodynamic conditions on the formation energies of intra(CO_3) CPDs. All of these results were obtained from ab initio-based IPDA calculations at T=800 K. For all CPDs, figures (c) and (d) display the minimum of formation energies over charge states for each (A ; μ(O)).

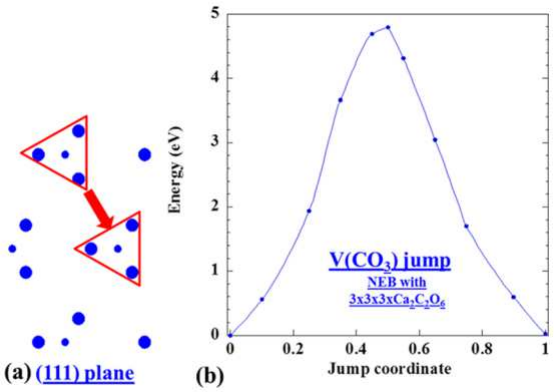

Figure 8. (a) Sketch of V(CO_3) jump between two neighboring CO_3 groups; (b) corresponding migration energy profile, obtained from ab initio calculations using the NEB technique with 3×3×3 $Ca_2C_2O_6$ image systems.

Turning toward V(CO), the situation is much more intricate than for V(CO_3), since even restricting to intra(CO_3) configurations, several types of V(CO) jumps have to be considered. The first, obvious type of jump is a V(CO) reorientation within a single CO_3 group noted CO_3a. Note that this CO_3a→CO_3a transition for V(CO) is the CPD counterpart of the previously studied $2N_{abs}$ jump (Figure 5a) for a single O vacancy. The NEB energy profile for this transition is displayed in Figure 9a, for two system sizes (2×2x2 or 2×2×3). Whatever the system size, it clearly indicates that the energy barrier for this CPD jump is very low, that is, E_m(V(CO), CO_3a→CO_3a)=0.16 eV (compare with $2N_{abs}$ jump of O vacancy in Table 1), and due to this easy trapping within CO_3 groups, V(CO) complexes should thus spend a large proportion of time performing such non diffusive reorientations. Conversely, diffusive jumps implying two neighboring CO_3 groups (noted CO_3a and CO_3b) are depicted in Figure 9b. As a remarkable result, no diffusive energy profile could be obtained by NEB for any of these transitions. In particular, although it might seem straightforward since it merely involves a rigid-body translation of the CPD, the "straight" transition depicted by the dashed-line green box of Figure 9b led to unrealistically high migration energy levels, as indicated by the NEB energy profile (displayed in Figure S4).

It is noticeable that this straight V(CO) jump was found to give rise to a rather stable intermediate state (only ∼0.5 eV above the stable V(CO) level) corresponding to a symmetrized configuration for the CO_3 group. For the reason of limited interatomic spacing in the $CaCO_3$ unit cell, the latter configuration however cannot be expected in perfect $CaCO_3$ and is thus probably induced by the vicinity of the V(CO) defect. The possible role of such symmetrized configurations in diffusion processes in $CaCO_3$ may deserve further investigations, which were left for future work. Finally, the other transitions investigated for V(CO) (full-line red boxes in Figure 9b) correspond to even less favorable situations due to the requirement of CPD reorientations along the profile entailing excessively close atoms during the jump (a trend confirmed by preliminary NEB calculations). On the whole, within the present work, we were not able to identify for V(CO) a diffusive transition with a reasonably low energy barrier. Since similar trends about the transitions of Figure 9b were reached using either 2×2×2 or 3×3×3 ab initio systems, this consistently leads to the conclusion that V(CO) should be discarded for diffusion in $CaCO_3$, at least within (111) planes.

Noticeably, our ab initio calculations on CPDs in $CaCO_3$ emphasize a striking contrast between good stability (low formation energies) and poor diffusion properties (high jump profiles). In particular, it is remarkable that the jump pro fi le for V(CO_3) presents a high (∼5 eV) energy barrier, a result apparently at odds with the important role put down to CO_3^{2-} ions in the literature on calcite. Since this jump profile was obtained for a rather large (3×3×3) ab initio supercell, this surprising result cannot be explained solely by spurious interactions between the jumping CPD and its periodic images. It should also be noted that all migration profiles in the present work were obtained for globally neutral systems, whereas local charges may stabilize CPDs (cf. Figure 7), as shown by our above study of CPD stability including charge effects. Thus, it cannot be excluded that some dynamic effect (namely, during the CPD jump) related to the local charge might be responsible for a strong lowering of the energy barrier for V(CO_3) jumps, and further investigations of this difficult issue would be relevant. As for V(CO), although we were not able to determine a reasonable migration energy for any diffusive jump within (111) planes, the conclusion is far less definite than for V(CO_3), and it cannot be excluded that such jumps may indeed occur through proper reorientations of V(CO), but the latter still remain to be identified, for instance by specific molecular dynamics simulations beyond the scope of this work.

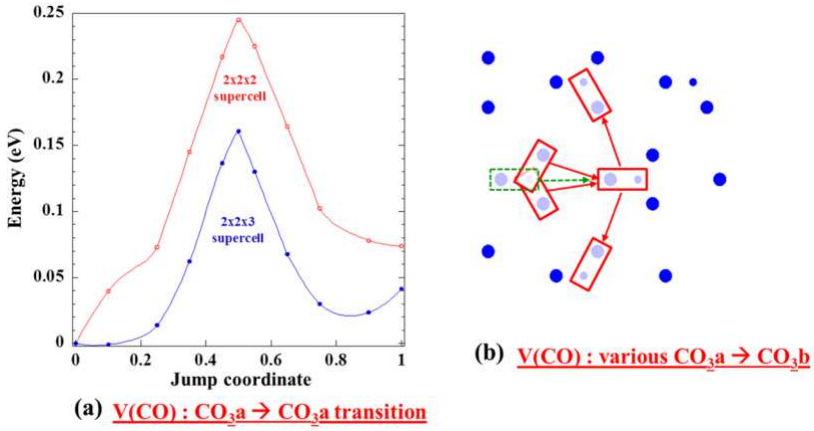

Figure 9. (a) NEB energy pro fi le for the (inherently non diffusive) CO_3a→CO_3a jump of V(CO) within a single CO_3 group, for two sizes of ab initio supercells; (b) sketch of various (possibly diffusive) CO_3a→CO_3b jumps of V(CO) between two neighboring CO_3 groups labeled CO_3a and CO_3b: boxes in full lines refer to four variants of the same jump, whereas the dashed-line box indicates another kind of CO_3a→CO_3b jump with a single variant, referred to as straight since it involves no reorientation of the CO migrating group (see also text and Figure S4).

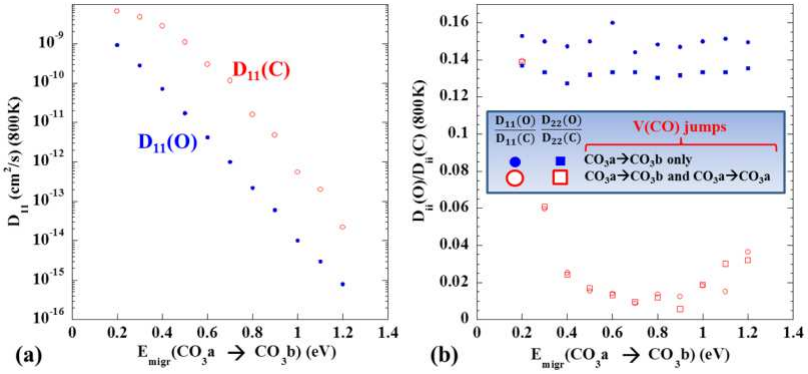

Figure 10. (a) Intra(111) plane C and O diffusion coefficients in calcite through the V(CO) mechanism, obtained from KMC simulations (100×100 unit cells): parametric study as a function of E_m(CO_3a→CO_3b) and using the ab initio value E_m(CO_3a→CO_3a)=0.16 eV (same notations as in Figure 9). (b) Corresponding D(O)/D(C) ratio, either neglecting (full symbols) or including (open symbols) CO_3a→CO_3a transitions within a single CO_3 group.

Since atomic transitions involving V(CO) CPDs conveniently allow for joint C and O diffusion, it is therefore of interest, even in the absence of a well-defined value for the migration energy of CO_3a→CO_3b jumps, to further investigate this mechanism by means of two-dimensional KMC simulations (cf. right part of Figure 1), using as input the migration energy E_m(CO_3a→CO_3a)=0.16 eV determined previously from ab initio calculations (Figure 9a) and keeping as a parameter the unknown migration energy of the CO_3a→CO_3b transition depicted in Figure 9b. The system used in these KMC simulations consisted of 100×100 2D unit cells, corresponding to V(CO) amounts within the [10^{-5};10^{-4}] range. While the ~1 eV formation energy for V(CO) read from Figure 7a would readily suggest a lower CPD amount (~5×10^{-7}), this discrepancy is immaterial for the present purpose: we mainly aim here at comparing V(CO)-mediated diffusion of C and O, without regard to the absolute magnitudes of the diffusion coefficients, since the latter depend on the unknown parameter

$E_m(CO_3a \rightarrow CO_3b)$. Figure 10a, which displays the results of these simulations, shows that both the carbon and oxygen V(CO)-mediated diffusion coefficients are strongly dependent on $E_m(CO_3a \rightarrow CO_3b)$, with C diffusion constantly 2 orders of magnitude above O diffusion. Figure 10b provides further details on these trends: by investigating the effect of $E_m(CO_3a \rightarrow CO_3a)$, it indicates that the low value of this parameter is directly responsible for the $D(O)/D(C) \sim 10^{-2}$ ratio. Therefore, easy V(CO) reorientations within the CO_3 groups lead to a strong lowering of O diffusion, and the V(CO) mechanism should thus be responsible for efficient C diffusion only. However, our study has revealed previously that the aforementioned O(int) and V(O) mechanisms should also be present, thus ensuring the wide oxygen diffusion required to convey this species to the internal interface where the carbonation reaction occurs.

4. DISCUSSION

It is instructive to compare the present theoretical study with previous experimental investigations on carbon and oxygen diffusion in calcite, especially the work[5] of Labotka et al. Investigating C and O diffusion at 800°C and between 1 and 2000 bar, these authors reached the conclusion that the oxygen diffusion coefficient D(O) is roughly constant (10^{-14}–10^{-13} cm^2/s) and D(C)−D(O) in this whole (T,P) range, whereas D(C) is strongly reduced (down to $\sim 10^{-16}$ cm^2/s) when P is increased up to 500 bar. Concerning oxygen diffusion, although we were interested in much lower pressures, our results are in rather good agreement with these experimental data, as regards (i) the order of magnitude of D(O), and (ii) the evidence of, at least, two mechanisms, probably ensuring good O mobility in a wide range of thermodynamic conditions. It should be noted that following the same analysis as above and keeping the perfect gas approximation for CO_2, higher pressures should correspond to an increase of the A parameter used in our work (A∼−23 eV rather than −24 or −25 eV). Conversely, these previous experimental results revealed that C diffusion may be more difficult than O diffusion since it is apparently much more sensitive to the thermodynamic conditions. It suggests that C diffusion may be strongly monitored by a single type of mechanism and thus rely on a single type of point defect probably disappearing when the pressure increases. This trend seems qualitatively consistent with our conclusion that complex point defects are present in a narrow range of chemical potentials. However, our simulations were not able to identify which complex may be active for C transport. In particular, it is surprising that our calculations point out the CO_3^{2-} carbonate ion as poorly mobile, whereas it is usually presented as a main vector for diffusion in calcite. Several causes may be invoked to explain this discrepancy, the first of which is a deficiency, when investigating energy barriers of the PBE exchange − correlation functional used for the present DFT calculations, possibly indicating unrealistic account of charge delocalization, since the latter are related to the choice of the density functional. Conversely, it is noticeable that this functional has demonstrated an overall satisfactory behavior for most point-defect properties in our study. Nevertheless, other factors, far beyond the scope of the present work, may be held responsible for a significant lowering or the saddle-point energy of the CO_3 vacancy, for example, dynamic effects related to anharmonic phonons or to local charges along the migration paths. Although extremely intricate, these important issues doubtlessly require further investigations to help reconcile experiments and simulations. In particular, complementary works might be useful to select, and perhaps optimize, an exchange − correlation functional best adapted to defects and diffusion in $CaCO_3$.

In the framework of better understanding the $CaO \leftrightarrow CaCO_3$ phase transformation, it is interesting to consider finally the implications of our work on the macroscopic matter transport properties

within a growing calcite layer. To this aim, it is logical to mention the so-called "BP" mechanism proposed by Bhatia and Perlmutter[7] and followed by par Sun,[6] relying on a hypothesis of opposite O^{2-} et CO_3^{2-} fluxes and which has been widely accepted in the literature to explain the growth of a $CaCO_3$ layer. As regards O^{2-}, our calculations tend to justify the role of this chemical species since they lead to a rather high oxygen diffusion coefficient, with values close to those obtained from experiments.[5] However, our work also suggests the possibility of a competition between the interstitial and vacancy mechanisms for O, a feature not taken into account in the aforementioned macroscopic mechanism.[7] More precisely, the profile of oxygen chemical potential μ(O) across the layer may have a critical influence: our results indicate that (i) if the thermodynamic conditions deduced from those at the outer interface (sufficiently "high" μ(O)) can be regarded as valid everywhere in the layer, then the interstitial mechanism should be the only one to be active, whereas (ii) a sufficiently μ(O) low value in the inner part of the layer may entail a change of mechanism (interstitial → vacancy) for some critical depth inside the layer, with possible consequences on the macroscopic modeling of $CaCO_3$ growth. As for carbon diffusion, in the BP mechanism it is supposed to occur through CO_3^{2-} ions, an assumption consistent with our study concluding that the diffusion of this element may require complex point defects. However, our results also point out the CO_3 vacancy complex as poorly mobile and less stable than its CO vacancy counterpart, and furthermore the presence of V(CO_3) implies that μ(O) might be sufficiently low everywhere, even at the outer interface where the thermodynamic conditions seem to make such features impossible. On the whole, these arguments deduced from the present work lead to the conclusion that C diffusion through V(CO_3) within the whole calcite layer is unrealistic. Further theoretical and experimental investigations would thus be very useful to elucidate these issues.

5. CONCLUSIONS

We have performed an atomic-scale theoretical study of diffusion in $CaCO_3$ calcite by means of ab initio calculations, together with analytical modeling or kinetic Monte Carlo simulations of the C and O diffusion tensors. We have demonstrated that, depending on the thermodynamic conditions, oxygen diffusion may be mediated by either an interstitial or a vacancy mechanism: O transport should therefore occur easily, in good agreement with previous experimental results. Conversely, our results point out completely different trends for carbon: although complex point defects such as V(CO) or V(CO_3) show remarkable stability (hence are potentially consistent with C diffusion), our DFT calculations also surprisingly indicate a low mobility for these complexes. While our results point out that further works may be required to identify the mechanisms responsible for carbon transport in calcite, they may also be a hint that bulk C diffusion in monocrystalline $CaCO_3$ is inefficient and readily overcome by intergranular diffusion, possibly involving the undissociated CO_2 molecule itself. Theoretical investigations of the CO_2 behavior in $CaCO_3$ model grain boundaries, as well as diffusion experiments on monocrystals, might be useful to check the validity of this hypothesis, which may offer a plausible alternative to the mechanism, frequently quoted in the literature on calcite, involving CO_3 carbonate groups.

■ ASSOCIATED CONTENT

Supporting Information

■ AUTHOR INFORMATION

Corresponding Author * E-mail: Remy.Besson@univ-lille.fr.

ORCID

Rémy Besson: 0000-0002-5270-8698

Loïc Favergeon: 0000-0001-8181-867X

Notes

The authors declare no competing financial interest.

■ ACKNOWLEDGMENTS

The authors thank the Centre de Ressources Informatiques (CRI) of the Université des Sciences et Technologies de Lille for computational facilities. The calculations in this work were also performed using MAGI, the HPC cluster of Sorbonne Paris Cité (SPC) University. The authors thank N. Greneche for his support on MAGI.

■ REFERENCES

(1) Besson, R.; Rocha Vargas, M.; Favergeon, L. CO_2 Adsorption on Calcium Oxide: An Atomic-Scale Simulation Study. Surf. Sci. 2012, 606, 490−195.

(2) Besson, R.; Favergeon, L. Atomic-Scale Study of Calcite Nucleation in Calcium Oxide. J. Phys. Chem. C 2013, 117, 8813−8821.

(3) Valverde, J. M.; Sanchez-Jimenez, P. E.; Perez-Maqueda, L. A. Limestone Calcination Nearby Equilibrium: Kinetics, CaO Crystal Structure, Sintering and Reactivity. J. Phys. Chem. C 2015, 119, 1623−1641.

(4) Valverde, J. M.; Medina, S. Crystallographic Transformation of Limestone during Calcination under CO 2 . Phys. Chem. Chem. Phys. 2015, 17, 21912−21926.

(5) Labotka, T. C.; Cole, D. R.; Riciputi, L. R.; Fayek, M. Diffusion of C and O in calcite from 0.1 to 200 MPa. Am. Mineral. 2004, 89, 799−806.

(6) Sun, Z.; Luo, S.; Qi, P.; Fan, L. Ionic Diffusion through Calcite ($CaCO_3$) Layer during the Reaction of CaO and CO 2 . Chem. Eng. Sci. 2012, 81, 164−168.

(7) Bhatia, S. K.; Perlmutter, D. D. Effect of the Product Layer on the Kinetics of the CO_2-Lime Reaction. AIChE J. 1983, 29, 79−86.

(8) Fisler, D. K.; Gale, J. D.; Cygan, R. T. A Shell Model for the Simulation of Rhombohedral Carbonate Minerals and their Point Defects. Am. Mineral. 2000, 85, 217−224.

(9) de Leeuw, N. H.; Cooper, T. G.; Nelson, C. J.; Mkhonto, D.; Ngoepe, P. E. Computer Simulation of Surfaces of Metals and Metal-Oxide Materials. In Computational Materials Science ; Catlow, R.,

Kotomin, E., Eds.; NATO Science Series, Series III: Computer and Systems Sciences; IOS Press, 2003; Vol. 187, pp 218−244.

(10) Rohl, A. L.; Wright, K.; Gale, J. D. Evidence from Surface Phonons for the (2×1) Reconstruction of the ($10\bar{1}$ 4) Surface of Calcite from Computer Simulation. Am. Mineral. 2003, 88, 921−925.

(11) Lardge, J. S.; Duffy, D. M.; Gillan, M. J.; Watkins, M. Ab initio Simulations of the Interaction between Water and Defects on the Calcite ($10\bar{1}$ 4) Surface. J. Phys. Chem. C 2010, 114, 2664−2668.

(12) Akiyama, T.; Nakamura, K.; Ito, T. Atomic and Electronic Structures of $CaCO_3$ Surfaces. Phys. Rev. B 2011, 84, No. 085428.

(13) Besson, R.; Favergeon, L. Understanding the Mechanisms of CaO Carbonation: Role of Point Defects in $CaCO_3$ by Atomic-Scale Simulations. J. Phys. Chem. C 2014, 118, 22583−22591.

(14) Kresse, G.; Furthmuller, J. Efficient Iterative Schemes for Ab Initio Total-Energy Calculations Using a Plane-Wave Basis Set. Phys. Rev. B 1996, 54, 11169−11186.

(15) Kresse, G.; Furthmuller, J. Efficiency of Ab Initio Total-Energy Calculations for Metals and Semiconductors Using a Plane-Wave Basis Set. Comput. Mater. Sci. 1996, 6, 15−50.

(16) Kresse, G.; Joubert, D. From Ultrasoft Pseudopotentials to the Projector Augmented-Wave Method. Phys. Rev. B 1999, 59, 1758−1775.

(17) Perdew, J. P.; Burke, K.; Ernzerhof, M. Generalized Gradient Approximation Made Simple. Phys. Rev. Lett. 1996, 77, 3865−3868.

(18) Besson, R. Point Defects in Multicomponent Ordered Alloys: Methodological Issues and Working Equations. Acta Mater. 2010, 58, 379−385.

(19) Bruneval, F.; Varvenne, C.; Crocombette, J.-P.; Clouet, E. Pressure, Relaxation Volume, and Elastic Interactions in Charged Simulation Cells. Phys. Rev. B 2015, 91, No. 024107.

(20) Tingaud, D.; Nardou, F.; Besson, R. Diffusion in Complex Ordered Alloys: Atomic-Scale Investigation of NiAl 3 . Phys. Rev. B 2010, 81, No. 174108.

(21) Besson, R.; Guyot, S.; Legris, A. Atomic-Scale Study of Diffusion in A15 Nb_3Sn. Phys. Rev. B 2007, 75, No. 054105.